Vidal, Y.; Villon, P. and Huerta, A., Locking in the incompressible limit: pseudo-divergence-free element free Galerkin, *Communications in Numerical Methods in Engineering*, Vol. 19, Issue 9, pp. 725-735, 2003

Locking in the incompressible limit: pseudo-divergence-free element free Galerkin

Yolanda Vidal[1,*], Pierre Villon[2] and Antonio Huerta[1]

[1] *Departament de Matemàtica Aplicada III, E.T.S. de Ingenieros de Caminos, Canales y Puertos, Universitat Politècnica de Catalunya, Jordi Girona 1, Barcelona E-08034, Spain*
[2] *Département Génie des Systèmes Mécaniques, Université de Technologie de Compiègne, Compiègne, France*

SUMMARY

Locking in finite elements has been a major concern since its early developments. It appears because poor numerical interpolation leads to an over-constrained system. This paper proposes a new formulation that asymptotically suppresses locking for the element free Galerkin (EFG) method in incompressible limit, i.e. the so-called volumetric locking. Originally it was claimed that EFG did not present volumetric locking. However, recently, performing a modal analysis, the senior author has shown that EFG presents volumetric locking. In fact, it is concluded that an increase of the dilation parameter attenuates, but never suppresses, the volumetric locking and that, as in standard finite elements, an increase in the order of reproducibility (interpolation degree) reduces the relative number of locking modes. Here an improved formulation of the EFG method is proposed in order to alleviate volumetric locking.

Diffuse derivatives are defined in the thesis of the second author and their convergence to the derivatives of the exact solution, when the radius of the support goes to zero (for a fixed dilation parameter), it is proved. Therefore, diffuse divergence converges to the exact divergence. Since the diffuse divergence-free condition can be imposed *a priori*, new interpolation functions are defined that asymptotically verify the incompressibility condition. Modal analysis and numerical results for classical benchmark tests in solids corroborate this issue.

KEY WORDS: incompressible locking; element free Galerkin; meshless; mesh free; diffuse derivatives

1. INTRODUCTION

In a recent paper [1] locking of the element free Galerkin (EFG) method near the incompressible limit, i.e. the so-called volumetric locking, has been studied. In particular, the standard EFG behaviour is compared with finite elements, bilinear and biquadratic interpolations. Locking of standard finite elements has been extensively studied and one can find in the literature several remedies to suppress or at least alleviate locking [2].

*Correspondence to: Y. Vidal, Deptament de Matemàtica Aplicada III, UPC, Jordi Girona 1, E-08034 Barcelona, Spain.

Contract/grant sponsor: Ministerio de Ciencia y Tecnología; contract/grant number: DPI2001-2204
Contract/grant sponsor: Ministerio de Ciencia y Tecnología; contract/grant number: REN2001-0925-C03-01

However, even recently [3] it was claimed that mesh-free methods did not exhibit volumetric locking. Now it is clear that this is not true. For instance, in Reference [4] the numerical inf–sup condition is used to analyse the EFG method. Moreover, several authors have studied the influence of the dilation parameter in locking phenomena, either by numerical experiments [4, 5] or by heuristic arguments [6] based on the constraint ratio proposed by Hughes [2]. Now it is clear [1] that the dilation parameter attenuates locking but does not suppress the locking modes and that, as in finite elements, an increase in the order of consistency decreases the number of locking modes. The remedies proposed in the literature are extensions of the methods developed for finite elements [4, 6].

Here a novel approach is explored. It consist in using interpolation functions that verify approximately the divergence-free restriction. These interpolating functions can be defined *a priori* and are independent of the particle distribution. Moreover, as the density of particles is increased (i.e. as the discretization is refined) the divergence-free condition is better approximated. This method is based on diffuse derivatives [7], which converge to the derivatives of the exact solution when the radius of the support goes to zero (for a fixed dilation parameter) [8].

2. DIFFUSE DERIVATIVES

2.1. Preliminaries of the EFG method

This section will not be devoted to develop or discuss mesh-free methods in detail or their relation with moving least-squares (MLS) interpolants. There are well-known references with excellent presentations of mesh-free methods, see for instance References [7, 9–12]. Here some basic notions will be recalled in order to introduce the notation and the approach employed in following sections.

The moving least-squares approach is based on the local (i.e. at any point $\boldsymbol{z}$ in the neighbourhood of $\boldsymbol{x}$) approximation of the unknown scalar function $u(\boldsymbol{z})$ by u^ρ as

$$u(\boldsymbol{z}) \simeq u^\rho(\boldsymbol{x},\boldsymbol{z}) = \mathbf{P}^{\mathsf{T}}(\boldsymbol{z})\mathbf{a}(\boldsymbol{x}) \quad \text{for } \boldsymbol{z} \text{ near } \boldsymbol{x} \tag{1}$$

where the coefficients $\mathbf{a}(\boldsymbol{x}) = \{\mathrm{a}_0(\boldsymbol{x}), \mathrm{a}_1(\boldsymbol{x}), \ldots, \mathrm{a}_l(\boldsymbol{x})\}^{\mathsf{T}}$ are not constant, they depend on point $\boldsymbol{x}$, and $\mathbf{P}(\boldsymbol{z}) = \{p_0(\boldsymbol{z}), p_1(\boldsymbol{z}), \ldots, p_l(\boldsymbol{z})\}^{\mathsf{T}}$ includes a complete basis of the subspace of polynomials of degree m. In one dimension, it is usual that $p_i(x)$ coincides with the monomials x^i, and, in this particular case, $l = m$. The coefficients $\mathbf{a}$ are obtained by the minimization of the functional $J_{\boldsymbol{x}}(\mathbf{a})$ centered in $\boldsymbol{x}$ and defined as

$$J_{\boldsymbol{x}}(\mathbf{a}) = \sum_{i \in I_{\boldsymbol{x}}} \phi(\boldsymbol{x}, \boldsymbol{x}_i)[u(\boldsymbol{x}_i) - \mathbf{P}(\boldsymbol{x}_i)\mathbf{a}(\boldsymbol{x})]^2 \tag{2}$$

where $\phi(\boldsymbol{x}, \boldsymbol{x}_i)$ is a weighting function (positive, even and with compact support) which characterizes the mesh-free method. For instance, if $\phi(\boldsymbol{x}, \boldsymbol{x}_i)$ is continuous together with its first k derivatives, the interpolation is also continuous together with its first k derivatives. The particles cover the computational domain Ω, $\Omega \subset \mathbb{R}^{n_{\mathrm{sd}}}$, and in particular a number of particles $\{\boldsymbol{x}_i\}_{i \in I_{\boldsymbol{x}}}$ belong to the support of $\phi(\boldsymbol{x}, \boldsymbol{x}_i)$. The minimization of $J_{\boldsymbol{x}}(\mathbf{a})$ induces the standard normal equations in a weighted least-squares problem

$$\mathbf{M}(\boldsymbol{x})\mathbf{a}(\boldsymbol{x}) = \sum_{i \in I_{\boldsymbol{x}}} \phi(\boldsymbol{x}, \boldsymbol{x}_i) u(\boldsymbol{x}_i) \mathbf{P}(\boldsymbol{x}_i) \tag{3}$$

where, as usual, the Gram matrix $\mathbf{M}(\boldsymbol{x})$ is the scalar product of the interpolation polynomials:

$$\mathbf{M}(\boldsymbol{x}) = \sum_{i \in I_x} \phi(\boldsymbol{x}, \boldsymbol{x}_i) \mathbf{P}(\boldsymbol{x}_i)^\mathsf{T} \mathbf{P}(\boldsymbol{x}_i) \tag{4}$$

That is,

$$\langle u, v \rangle = \sum_{i \in I_x} \phi(\boldsymbol{x}, \boldsymbol{x}_i) u(\boldsymbol{x}_i) v(\boldsymbol{x}_i) \tag{5}$$

must define a discrete scalar product. Thus, several conditions on the particle distribution are implicitly assumed, see for instance Reference [13].

Once the normal equations are solved (3) the coefficients $\mathbf{a}$ are substituted in (1). Since the weighting function ϕ usually favours the central point $\boldsymbol{x}$, it seems reasonable to assume that such an approximation is more accurate precisely at $\boldsymbol{z} = \boldsymbol{x}$ and thus approximation (1) is particularized at $\boldsymbol{x}$, that is,

$$u(\boldsymbol{x}) \simeq u^\rho(\boldsymbol{x}) = \mathbf{P}^\mathsf{T}(\boldsymbol{x}) \mathbf{a}(\boldsymbol{x}) = \mathbf{P}^\mathsf{T}(\boldsymbol{x}) \mathbf{M}^{-1}(\boldsymbol{x}) \sum_{i \in I_x} \phi(\boldsymbol{x}, \boldsymbol{x}_i) u(\boldsymbol{x}_i) \mathbf{P}(\boldsymbol{x}_i) \tag{6}$$

This expression can also be written in a standard interpolation form

$$u^\rho(\boldsymbol{x}) = \sum_{i \in I_x} N_i^\rho(\boldsymbol{x}) u(\boldsymbol{x}_i) = \sum_{i \in I_x} [\phi(\boldsymbol{x}, \boldsymbol{x}_i) \mathbf{P}^\mathsf{T}(\boldsymbol{x}) \mathbf{M}^{-1}(\boldsymbol{x}) \mathbf{P}(\boldsymbol{x}_i)] u(\boldsymbol{x}_i) \tag{7}$$

2.2. *The diffuse derivative*

The approximation of the derivative of u is the derivative of u^ρ. This requires to derive (6), that is,

$$\frac{\partial u}{\partial x_i} \simeq \frac{\partial u^\rho}{\partial x_i} = \frac{\partial \mathbf{P}^\mathsf{T}}{\partial x_i} \mathbf{a}(\boldsymbol{x}) + \mathbf{P}^\mathsf{T} \frac{\partial \mathbf{a}}{\partial x_i} \quad \text{for } i = 1, \ldots, n_{\mathtt{sd}} \tag{8}$$

Note that the derivative of the polynomials in $\mathbf{P}$ is trivial but the derivative of the coefficients $\mathbf{a}$ requires the resolution of a linear system of equations with the same matrix $\mathbf{M}$, see Reference [14]. Moreover, the derivatives of the polynomials can be done *a priori* but the derivatives of the coefficients require the knowledge of the cloud of particles surrounding each point $\boldsymbol{x}$.

Thus the concept of diffuse derivative, see References [7, 8], defined as

$$\frac{\delta u^\rho}{\delta x_i} = \left. \frac{\partial u^\rho}{\partial z_i} \right|_{z=x} = \left. \frac{\partial \mathbf{P}^\mathsf{T}}{\partial z_i} \right|_{z=x} \mathbf{a}(\boldsymbol{x}) = \frac{\partial \mathbf{P}^\mathsf{T}}{\partial x_i} \mathbf{a}(\boldsymbol{x}) \quad \text{for } i = 1, \ldots, n_{\mathtt{sd}} \tag{9}$$

is from a computational cost point of view an interesting alternative to (8). Moreover, the diffuse derivative converges at optimal rate to the derivative of u, see the demonstration in Reference [8]. For an approximation u^ρ to u with an order of consistency m (i.e. $\mathbf{P}$ includes a complete base of the subspace of polynomials of degree m), then

$$\left\| \frac{\partial^k u}{\partial x_i^k} - \frac{\delta^k u^\rho}{\delta x_i^k} \right\|_\infty \leqslant C(\boldsymbol{x}) \frac{\rho^{m+1-k}}{(m+1)!} \quad \forall k = 0, \ldots, m \text{ and for } i = 1, \ldots, n_{\mathtt{sd}} \tag{10}$$

3. PSEUDO-DIVERGENCE FREE CONDITION

3.1. Diffuse divergence

In the previous section, the diffuse derivative was introduced and it was recalled that it converges to the actual derivative as $\rho \to 0$. Moreover, diffuse derivatives only act on the polynomials $\mathbf{P}$. Incompressible computations require that the approximating field must be divergence free. That is, the solution $\boldsymbol{u}(\boldsymbol{x})$, now a vector $\boldsymbol{u} : \mathbb{R}^{n_{\mathsf{sd}}} \to \mathbb{R}^{n_{\mathsf{sd}}}$, verifies $\nabla \cdot \boldsymbol{u} = 0$, and the approximation $\boldsymbol{u}^\rho(\boldsymbol{x})$ should also be divergence free. This condition, however, depends on the interpolation space. Here, instead of requiring a divergence-free interpolation, the diffuse divergence of the approximation

$$\boldsymbol{u}^\rho = \begin{pmatrix} u_1^\rho \\ \vdots \\ u_{n_{\mathsf{sd}}}^\rho \end{pmatrix} = \begin{pmatrix} \mathbf{P}^\mathsf{T}\mathbf{a}_1 \\ \vdots \\ \mathbf{P}^\mathsf{T}\,\mathbf{a}_{n_{\mathsf{sd}}} \end{pmatrix} = \begin{pmatrix} p_0(\boldsymbol{x})\mathbf{I}_{n_{\mathsf{sd}}} & p_1(\boldsymbol{x})\mathbf{I}_{n_{\mathsf{sd}}} & \cdots & p_l(\boldsymbol{x})\mathbf{I}_{n_{\mathsf{sd}}} \end{pmatrix} \begin{pmatrix} \mathbf{c}_0(\boldsymbol{x}) \\ \mathbf{c}_1(\boldsymbol{x}) \\ \vdots \\ \mathbf{c}_l(\boldsymbol{x}) \end{pmatrix} = \mathbf{Q}^\mathsf{T}\mathbf{c} \qquad (11)$$

is imposed equal to zero, i.e.

$$\nabla^\delta \cdot \boldsymbol{u}^\rho = \sum_{i=1}^{n_{\mathsf{sd}}} \frac{\delta \boldsymbol{u}^\rho}{\delta x_i} = \sum_{i=1}^{n_{\mathsf{sd}}} \frac{\partial \mathbf{P}^\mathsf{T}}{\partial x_i}\mathbf{a}_i(\boldsymbol{x}) = (\nabla \cdot \mathbf{Q}^\mathsf{T}(\boldsymbol{x}))\mathbf{c}(\boldsymbol{x}) = 0 \qquad (12)$$

Note that $\mathbf{I}_{n_{\mathsf{sd}}}$ is the identity matrix of order n_{sd} and the coefficients have been rearranged as

$$\mathbf{c}^\mathsf{T} = \Bigg(\underbrace{\mathrm{a}_{0,1} \cdots \mathrm{a}_{0,n_{\mathsf{sd}}}}_{\mathbf{c}_0^\mathsf{T}(\boldsymbol{x})} \; \underbrace{\mathrm{a}_{1,1} \cdots \mathrm{a}_{1,n_{\mathsf{sd}}}}_{\mathbf{c}_1^\mathsf{T}(\boldsymbol{x})} \cdots \underbrace{\mathrm{a}_{l,1} \cdots \mathrm{a}_{l,n_{\mathsf{sd}}}}_{\mathbf{c}_l^\mathsf{T}(\boldsymbol{x})} \Bigg) \qquad (13)$$

Equation (12) must hold at each point $\boldsymbol{x}$ and for any approximation. Thus appropriate interpolation functions, $\mathbf{Q}$, must be defined in order to verify (12) and thus ensure asymptotically a divergence-free interpolation (i.e. the divergence-free condition is fulfilled as $\rho \to 0$).

3.2. A 2D pseudo-divergence free interpolation

The previous concepts are particularized for a two-dimensional case and allow to define the pseudo-divergence-free interpolation functions. Suppose for instance that consistency of order two is desired, then $\mathbf{P}^\mathsf{T} = \{1, x_1, x_2, x_1^2, x_1x_2, x_2^2\}$, thus

$$\mathbf{Q}^\mathsf{T} = \begin{pmatrix} 1 & 0 & x_1 & 0 & x_2 & 0 & x_1^2/2 & 0 & x_1x_2 & 0 & x_2^2/2 & 0 \\ 0 & 1 & 0 & x_1 & 0 & x_2 & 0 & x_1^2/2 & 0 & x_1x_2 & 0 & x_2^2/2 \end{pmatrix} \qquad (14)$$

and

$$\mathbf{c}^\mathsf{T} = (\mathrm{a}_{0,1}\;\; \mathrm{a}_{0,2}\;\; \mathrm{a}_{1,1}\;\; \mathrm{a}_{1,2}\;\; \mathrm{a}_{2,1}\;\; \mathrm{a}_{2,2}\;\; \mathrm{a}_{3,1}\;\; \mathrm{a}_{3,2}\;\; \mathrm{a}_{4,1}\;\; \mathrm{a}_{4,2}\;\; \mathrm{a}_{5,1}\;\; \mathrm{a}_{5,2}) \qquad (15)$$

The pseudo-divergence-free condition (2) is, in this case, written as

$$\nabla^\delta \cdot \boldsymbol{u}^\rho = \frac{\partial \mathbf{P}^\mathsf{T}}{\partial x_1}\mathbf{a}_1 + \frac{\partial \mathbf{P}^\mathsf{T}}{\partial x_2}\mathbf{a}_2 = 0 \qquad (16)$$

which implies

$$(\mathrm{a}_{1,1}+\mathrm{a}_{2,2})+x_1(\mathrm{a}_{3,1}+\mathrm{a}_{4,2})+x_2(\mathrm{a}_{4,1}+\mathrm{a}_{5,2})=0 \tag{17}$$

and consequently,

$$\mathrm{a}_{1,1}+\mathrm{a}_{2,2}=0,\quad \mathrm{a}_{3,1}+\mathrm{a}_{4,2}=0,\quad \mathrm{a}_{4,1}+\mathrm{a}_{5,2}=0 \tag{18}$$

The influence of these three restrictions in the interpolation functions (14) can be viewed as follows:

$$\begin{pmatrix} 1 & 0 & x_1 & 0 & x_2 & 0 & x_1^2/2 & 0 & x_1x_2 & 0 & x_2^2/2 & 0 \\ 0 & 1 & -x_2 & x_1 & 0 & 0 & -x_1x_2 & x_1^2/2 & -x_2^2/2 & 0 & 0 & 0 \end{pmatrix} \tag{19}$$

where one should note that the coefficients in the x_1 and x_2 directions are now coupled and that the total number of degrees of freedom has decreased.

3.3. The pseudo-divergence-free EFG method

Using (19), let $\mathbf{Q}_\delta$ be the new interpolation matrix (where obviously the unnecessary columns have been removed). The interpolation is then defined as

$$\boldsymbol{u}(\boldsymbol{z})\simeq\boldsymbol{u}^\rho(\boldsymbol{x},\boldsymbol{z})=\begin{pmatrix} u_1^\rho(\boldsymbol{x},\boldsymbol{z}) \\ u_2^\rho(\boldsymbol{x},\boldsymbol{z}) \end{pmatrix}=\mathbf{Q}_\delta^{\mathsf{T}}(\boldsymbol{z})\mathbf{c}(\boldsymbol{x}) \tag{20}$$

The vector version of the discrete scalar product defined in (5),

$$\langle\boldsymbol{u},\boldsymbol{v}\rangle=\sum_{i\in I_x}\phi(\boldsymbol{x},\boldsymbol{x}_i)\boldsymbol{u}^{\mathsf{T}}(\boldsymbol{x}_i)\boldsymbol{v}(\boldsymbol{x}_i) \tag{21}$$

allows now to reproduce the MLS approximation. Thus, at each point $\boldsymbol{x}$ the normal equations should be solved, see (3),

$$\mathbf{M}(\boldsymbol{x})\mathbf{c}(\boldsymbol{x})=\langle u,\mathbf{Q}_\delta\rangle\quad \text{with } \mathbf{M}(\boldsymbol{x}):=\langle\mathbf{Q}_\delta,\mathbf{Q}_\delta\rangle \tag{22}$$

Thus, as previously, the coefficients $\mathbf{c}$ are substituted in (20) and the approximation is particularized at $\boldsymbol{z}=\boldsymbol{x}$. Then, Equation (6) becomes

$$\boldsymbol{u}(\boldsymbol{x})\simeq\boldsymbol{u}^\rho(\boldsymbol{x})=\mathbf{Q}_\delta^{\mathsf{T}}(\boldsymbol{x})\mathbf{c}(\boldsymbol{x})=\mathbf{Q}_\delta^{\mathsf{T}}(\boldsymbol{x})\mathbf{M}^{-1}(\boldsymbol{x})\langle u,\mathbf{Q}_\delta\rangle \tag{23}$$

and a final expression similar to (7) can be found as

$$\boldsymbol{u}^\rho(\boldsymbol{x})=\sum_{i\in I_x}\mathbf{N}_i^\rho(\boldsymbol{x})\boldsymbol{u}(\boldsymbol{x}_i)=\sum_{i\in I_x}[\phi(\boldsymbol{x},\boldsymbol{x}_i)\mathbf{Q}_\delta^{\mathsf{T}}(\boldsymbol{x})\mathbf{M}^{-1}(\boldsymbol{x})\mathbf{Q}_\delta(\boldsymbol{x}_i)]\boldsymbol{u}(\boldsymbol{x}_i) \tag{24}$$

It is important to note that the matrix of interpolation functions $\mathbf{N}_i^\rho$ is now a full matrix not a diagonal one as standard EFG would induce in this non-scalar problem. This is due to the fact that the two components of the solution are linked by the incompressibility restriction.

4. MODAL ANALYSIS

4.1. Preliminaries

The modal analysis presented here follows the same rationale originally presented in Reference [1]. It is restricted to small deformations, namely $\nabla^s \boldsymbol{u}$, where $\boldsymbol{u}$ is the displacement and ∇^s the symmetric gradient, i.e. $\nabla^s = \frac{1}{2}(\nabla^T + \nabla)$. Moreover, linear elastic isotropic materials under plane strain conditions are considered. Dirichlet boundary conditions are imposed on Γ_D, a traction $\boldsymbol{h}$ is prescribed along the Neumann boundary Γ_N and there is a body force $\boldsymbol{f}$. Thus, the problem that needs to be solved may be stated as, solve for $\boldsymbol{u} \in [H^1_{\Gamma_D}]^2$ such that

$$\frac{E}{1+v}\int_\Omega \nabla^s \boldsymbol{v} : \nabla^s \boldsymbol{u}\, d\Omega + \frac{Ev}{(1+v)(1-2v)}\int_\Omega (\nabla\cdot \boldsymbol{v})(\nabla\cdot\boldsymbol{u})\, d\Omega = \int_\Omega \boldsymbol{f}\cdot\boldsymbol{v}\, d\Omega + \int_{\Gamma_N} \boldsymbol{h}\cdot\boldsymbol{v}\, d\Gamma \quad \forall \boldsymbol{v} \in [H^1_{0,\Gamma_D}]^2 \tag{25}$$

In this equation, the standard vector subspaces of H^1 are employed for the solution $\boldsymbol{u}$

$$[H^1_{\Gamma_D}]^2 := \{\boldsymbol{u} \in [H^1]^2 \mid \boldsymbol{u} = \boldsymbol{u}_D \text{ on } \Gamma_D\}$$

(Dirichlet conditions, $\boldsymbol{u}_D$, are automatically satisfied) and for the test functions $\boldsymbol{v}$

$$[H^1_{0,\Gamma_D}]^2 := \{\boldsymbol{v} \in [H^1]^2 \mid \boldsymbol{v} = \boldsymbol{0} \text{ on } \Gamma_D\}$$

(zero values are imposed along Γ_D).

This equation shows the inherent difficulties of the incompressible limit. The standard *a priori* error estimate emanating from (25) and based on the energy norm, which is induced by the LHS of (25), is

$$\|\boldsymbol{u} - \boldsymbol{u}_h\| \leqslant \inf_{\boldsymbol{w}\in\mathscr{S}_h} \|\boldsymbol{u} - \boldsymbol{w}\| \leqslant C_{\boldsymbol{u},v,p} h^{f(p)} \tag{26}$$

where $\mathscr{S}_h$ is the finite dimensional subspace of $[H^1_{\Gamma_D}]^2$ in which the approximation $\boldsymbol{u}_h$ is sought, $C_{\boldsymbol{u},v,p}$ is a constant independent of h (characteristic size of the mesh), and $f(p)$ is a positive monotone function of p (degree of the polynomials used for the interpolation). The subindices of the constant C indicate that it depends on the Poisson ratio, the order of the interpolation and the exact solution itself.

From (25) one can observe the difficulties of the energy norm to produce a small infimum in (26) for values of v close to 0.5. In fact, in order to have finite values of the energy norm the divergence-free condition must be enforced in the continuum case, i.e. $\nabla\cdot\boldsymbol{u} = 0$ for $\boldsymbol{u} \in [H^1_{\Gamma_D}]^2$, and also in the finite-dimensional space, i.e. $\nabla\cdot\boldsymbol{u}_h = 0$ for $\boldsymbol{u}_h \in \mathscr{S}_h \subset [H^1_{\Gamma_D}]^2$. In fact, locking will occur when the approximation space $\mathscr{S}_h$ is not rich enough for the approximation to verify the divergence-free condition.

Under these conditions, it is evident that locking may be studied from the LHS of (25). This is the basis for the modal analysis of locking. The discrete eigenfunctions (the eigenvectors) corresponding to the LHS of (25) are computed because they completely describe, in the corresponding space, the behaviour of the bilinear operator induced by this LHS.

In computational mechanics it is standard to write the strain, $\boldsymbol{\varepsilon}$, and the stress, $\boldsymbol{\sigma}$, tensors in vector form. Moreover, under the assumptions already discussed, they are related as

$$\boldsymbol{\varepsilon} = \mathbf{B}\mathbf{d}, \quad \boldsymbol{\sigma} = \mathbf{C}\boldsymbol{\varepsilon}, \quad \mathbf{C} = \frac{E}{(1+\nu)(1-2\nu)} \begin{pmatrix} 1-\nu & \nu & 0 \\ \nu & 1-\nu & 0 \\ 0 & 0 & \dfrac{1-2\nu}{2} \end{pmatrix}$$

Where $\mathbf{d}$ is the vector of nodal displacements (the coefficients corresponding to the approximation $\boldsymbol{u}_h$ in the base of $\mathscr{S}_h$), and $\mathbf{B}$ is the standard matrix relating displacements and strains. Then, the stiffness matrix can be computed as usual

$$\mathbf{K} = \int_\Omega \mathbf{B}^{\mathsf{T}}\mathbf{C}\mathbf{B}\,\mathrm{d}\Omega$$

The modal analysis presented in the following is based on $\mathbf{K}$, which is naturally related to the energy norm in the finite-dimensional interpolation space, $\mathscr{S}_h$, defined by the finite elements employed (and characterized by $\mathbf{B}$).

4.2. Comparing EFG and pseudo-divergence-free EFG

The incompressible limit is studied by evaluating the eigenvalues associated to each mode as the Poisson ratio, ν, tends to 0.5. As in Reference [1] the logarithm of the eigenvalue is plotted as a function of the logarithm of $0.5-\nu$. Then each mode is classified in three groups: (1) modes that do not present any locking behaviour, (2) modes that do have physical locking, i.e. the eigenvalue goes to infinity because it is a volumetric mode, and (3) modes associated to non-physical locking, i.e. the eigenvalue goes to infinity but there is no volume variation. In the latter case, the displacement field conserves the total area but suffers from non-physical locking. The interpolation space is not rich enough to ensure the divergence-free condition. In fact these modes do verify that

$$\int_\square \boldsymbol{\nabla}\cdot\boldsymbol{u}_h\,\mathrm{d}\boldsymbol{x} = 0$$

but do not comply with the local divergence-free condition. This is clearly a non-physical locking behaviour.

The modal analysis is performed on a distribution of 3×3 particles and for bilinear consistency, i.e. $\mathbf{P} = \{1, x_1, x_2, x_1 x_2\}^{\mathsf{T}}$. Figures 1 and 2 show the modes already classified for two different dilation parameters, $\rho/h = 1.2$ and 2.2. And Figure 3 compares the eigenvalues obtained by standard EFG and the pseudo-divergence-free interpolation for two particular non-physical locking modes with $\rho/h = 1.2$, 2.2 and 3.2. Note first that the pseudo-divergence-free interpolation has not suppresses the non-physical locking modes. Thus, for a fixed dilation parameter ρ variations on the ratio ρ/h do not suppress locking. Indeed, the influence of locking is reduced because the eigenvalue is decreased. That is, the energy associated to the locking mode is decreased and this attenuates the volumetric locking. Nevertheless, in the incompressible limit locking will still be present and it may induce useless numerical results.

This results should be expected. The convergence of the diffuse derivative see (10) is ensured as ρ approaches zero for a ratio ρ/h kept constant. In other words, convergence is ensured as the interpolation is refined. This is analysed in Figure 4 for the non-physical locking

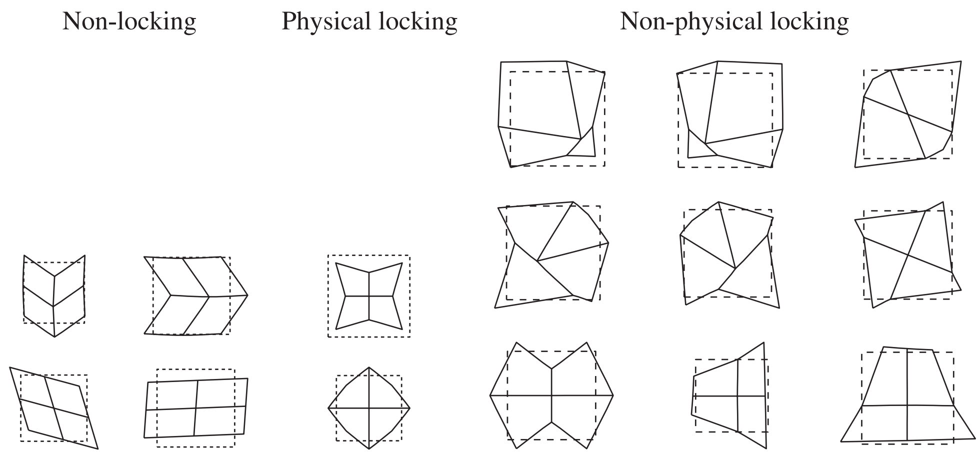

Figure 1. Modes for a 3×3 distribution of particles with bilinear consistency and $\rho/h = 1.2$.

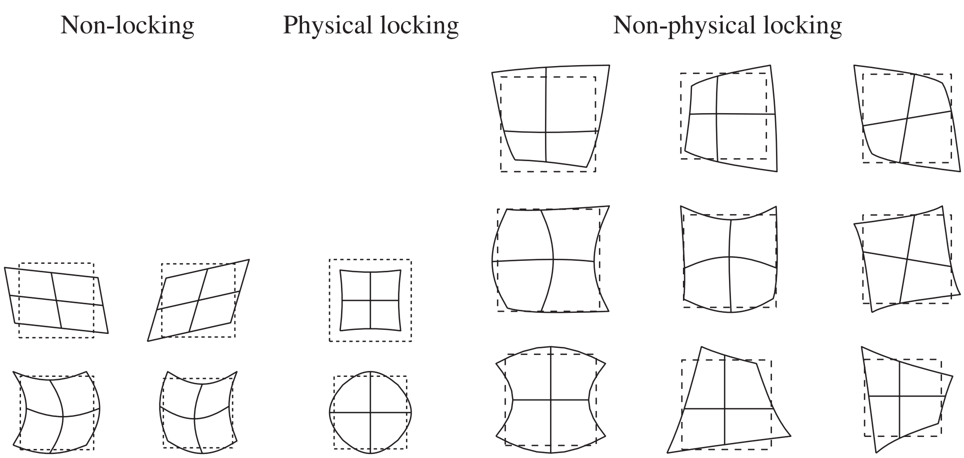

Figure 2. Modes for a 3×3 distribution of particles with bilinear consistency and $\rho/h = 2.2$.

mode that presents the largest eigenvalue (the first mode to spoil the approximation). This results are obtained for the ‘worst’ dilation parameter, $\rho/h = 1.2$, that is the one that induces results more similar to bilinear finite elements. Three different values of ρ are tested, $\rho = 0.60$, 0.24 and 0.15. It is important to note that as ρ decreases the eigenvalue also decreases (and drastically, the scale is logarithmic). Thus, as ρ decreases the influence of locking attenuates. Moreover, and more importantly, the slope of the curve also decreases as ρ goes to zero (note that for standard EFG the slope remains constant). Thus, in the limit, as expected, the interpolation is divergence free. Note that for $\rho = 0.15$ and $\nu = 0.5 - 10^{-11}$ the eigenvalue has been reduced in more than three orders of magnitude.

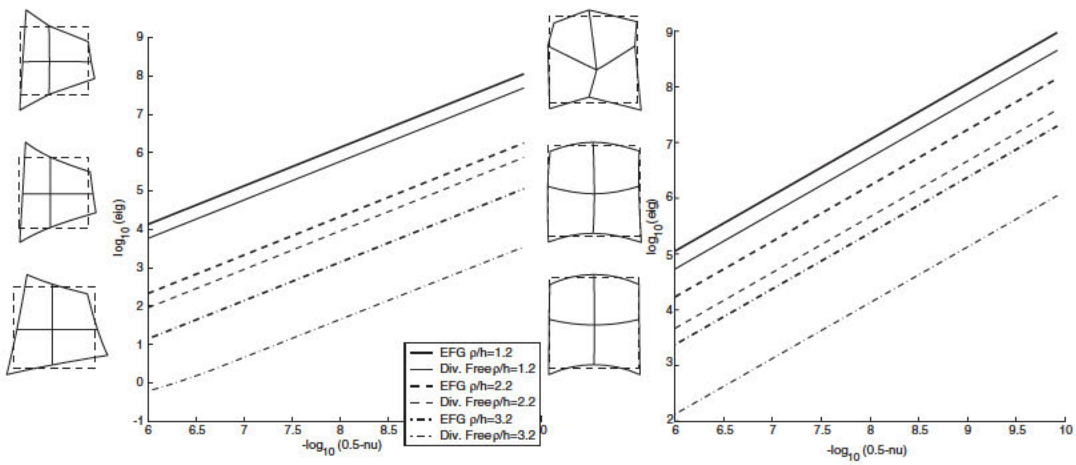

Figure 3. Variation of the eigenvalue as ν goes to 0.5 for the same non-physical locking mode with $\rho/h = 1.2$, 2.2 and 3.2. EFG results (thick lines) and pseudo-divergence-free interpolations (thin lines).

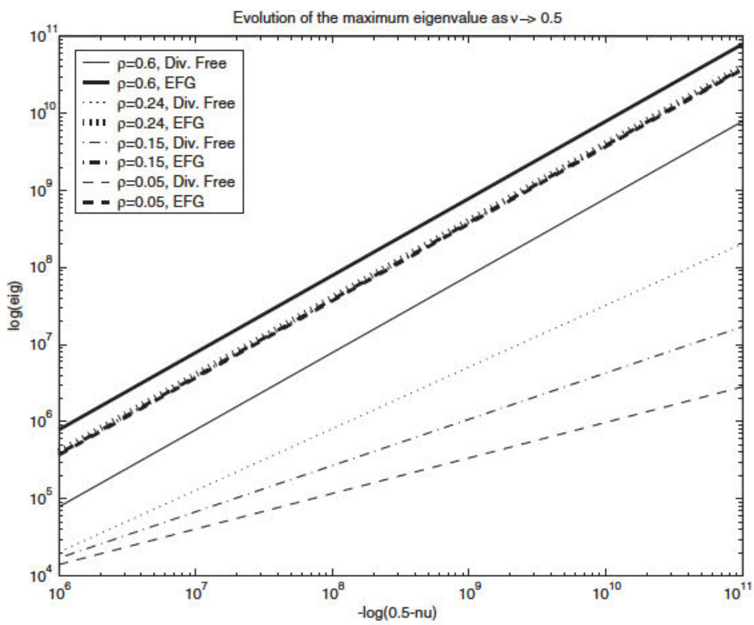

Figure 4. Variation of the maximum eigenvalue as ν goes to 0.5, EFG results (thick lines) and pseudo-divergence-free interpolations (thin lines).

5. NUMERICAL EXAMPLES

5.1. The cantilever beam

A beam with linear isotropic material, under plane strain conditions and with a parabolic traction applied to the free end is considered, as shown in Figure 5. Displacements in both

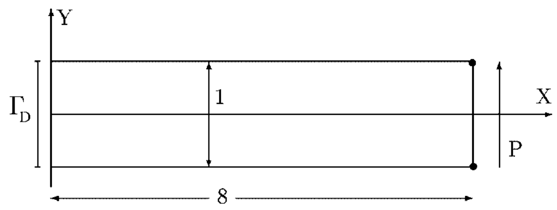

Figure 5. Cantilever beam problem.

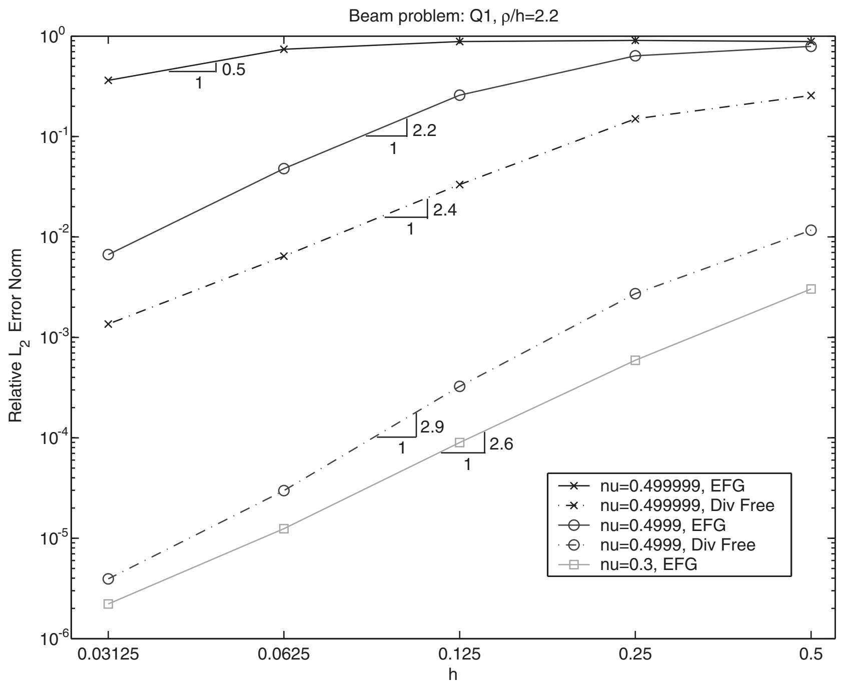

Figure 6. Cantilever beam with bilinear consistency and $\rho/h = 2.2$.

directions are prescribed at Γ_D. The prescribed displacements and the applied traction are such that the solution is known [2, 4]:

$$u_1 = -2\,\frac{1-\nu^2}{E}\,y\left[(48-3x_1)x_1 + \left(2+\frac{\nu}{1-\nu}\right)(x_2^2-0.25)\right]$$

$$u_2 = 2\,\frac{1-\nu^2}{E}\left[3\,\frac{\nu}{1-\nu}\,x_2^2(8-x_1) + \left(4+5\,\frac{\nu}{1-\nu}\right)\frac{x_1}{4} + (24-x_1)x_1^2\right]$$

$$\sigma_{11} = -12x_2(8-x_1), \quad \sigma_{22} = 0, \quad \sigma_{12} = 6(0.25-x_2^2)$$

The problem is solved with uniform distributions of particles. Figure 6 shows the relative L_2 error in displacements for $\nu = 0.3$, $0.5 - 10^{-4}$ and $0.5 - 10^{-6}$. Results are shown for bilinear consistency and $\rho/h = 2.2$. The EFG results are compared with the pseudo-divergence-free interpolation. For EFG the typical convergence rates are obtained when $v = 0.3$, but, as expected, results degrade as v approaches the incompressible limit 0.5. However, the pseudo-divergence free interpolation is able to reproduce the theoretical rate of convergence even for a nearly incompressible case $v = 0.5 - 10^{-6}$ and a moderately fine discretization ($h < 0.25$, i.e. $\rho < 0.55$).

6. CONCLUSIONS

An improved formulation of the EFG method is proposed in order to alleviate volumetric locking. It is based on a pseudo-divergence-free interpolation, which asymptotically verifies the incompressibility condition and is defined *a priori*. This interpolation is obtained imposing a zero diffuse divergence. Diffuse derivatives converge to the derivatives of the exact solution when the discretization is refined. Therefore, the diffuse divergence converges to the exact divergence. Modal analysis and a numerical results for a classical benchmark tests in solids corroborate this issue.

REFERENCES

1. Huerta A, Fernández-Méndez S. Locking in the incompressible limit for the Element free Galerkin method. *International Journal for Numerical Methods in Engineering* 2001; **51**(11):1361–1383.
2. Hughes TJR. *The Finite Element Method, Linear Static and Dynamic Analysis*. Prentice-Hall: Englewood Cliffs, NJ, 1987.
3. Zhu T, Atluri SN. A modified collocation method and a penalty formulation for enforcing the essential boundary conditions in the element free Galerkin method. *Computational Mechanics* 1998; **21**:211–222.
4. Dolbow J, Belytschko T. Volumetric locking in the element free Galerkin method. *International Journal for Numerical Methods in Engineering* 1999; **46**:925–942.
5. Askes H, de Borst R, Heeres O. Conditions for locking-free elasto-plastic analyses in the element free Galerkin method. *Computer Methods in Applied Mechanics and Engineering* 1999; **173**:99–109.
6. Chen J, Yoon S, Wang H, Liu WK. *Computer Methods in Applied Mechanics and Engineering* 2000; **181**:117–145.
7. Nayroles B, Touzot G, Villon P. Generating the finite element method: diffuse approximation and diffuse elements. *Computational Mechanics* 1992; **10**:307–318.
8. Villon P. Contribution à l'optimisation. *Thèse présentée pour l'obtention du grade de Docteur d'État*, Université de Technologie de Compiègne, France, 1991.
9. Belytschko T, Krongauz Y, Organ D, Fleming M, Krysl P. Meshless methods: an overview and recent developments. *Computer Methods in Applied Mechanics and Engineering* 1996; **139**:3–47.
10. Liu WK, Belytschko T, Oden JT (eds). Meshless methods. *Computer Methods in Applied Mechanics and Engineering* 1996; **139**:1–440.
11. Liu WK, Chen Y, Jun S, Chen JS, Belytschko T, Pan C, Uras RA, Chang CT. Overview and applications of the reproducing kernel particle methods. *Archives of Computational Methods in Engineering, State of the Art Reviews* 1996; **3**:3–80.
12. Liu WK, Li S, Belytschko T. Moving least square reproducing kernel methods. (I) Methodology and convergence. *Computer Methods in Applied Mechanics and Engineering* 2000; **143**:113–154.
13. Huerta A, Fernández-Méndez S. Enrichment and coupling of the finite element and meshless methods. *International Journal for Numerical Methods in Engineering* 2000; **48**:1615–1636.
14. Belytschko T, Krongauz Y, Fleming M, Organ D, Liu WK. Smoothing and accelerated computations in the element free Galerkin method. *Journal of Computational and Applied Mathematics* 1996; **74**:111–126.